Believe It or Not: Incorporating Relative Time Delay and Magnification Distributions Predicted by Lens Models into Ranking Possible Sub-Threshold, Strongly-Lensed Candidates

Haley Boswell[a]

(Dated: September 4, 2023)

We consider the possibility of gravitationally lensed pairs of gravitational waves, a phenomenon that has predominantly been studied in regard to electromagnetic waves. Under the strong lensing hypothesis, lensed gravitational waves from the same source are identical in waveform apart from a relative arrival time delay, an overall scaling factor in amplitude and a phase shift. It is possible that strong lensing produces magnified, super-threshold events that are registered as a trigger and demagnified, subthreshold events that get buried in the noise background. To remedy this, we search for subthreshold triggers using the gstLAL-based TargetEd Subthreshold Lensing SeArch (TESLA) pipeline, which considers the catalog of registered gravitational waves as potential lensed, super-threshold events. In this research, we incorporate a post-processing search for sub-threshold counterparts using a ranking statistic calculation based on the time delay and magnification probability distributions for a given lens model.

INTRODUCTION

While the study of gravitational lensing of light has been confirmed and widely studied, the possibility of gravitational lensed gravitational waves is still being explored. After analyzing data from the first half of LIGO/VIRGO's third observing run (O3a), the LVK collaboration (LIGO, VIRGO and KAGRA) concluded that there was no presence of strong lensing of gravitational waves (GWs)[1]. However, lensed counterparts are likely overlooked due to the effects of demagnification in signal amplitude. The accuracy and impact of our analyses of celestial bodies, their interactions, and spacetime itself will drastically improve when strong lensing of GWs is successfully identified. This includes better estimations of source parameters such as red-shift and chirp mass given the possibility of joint parameter estimation, or using multiple signals from the same source to better constrain the possible values. Additionally, while the distribution of dark matter is traditionally analyzed using its lensing effect of a background source's light, gravitational lensing of gravitational waves will expand this search to include lensed gravitational waves from less visible sources such as merging black holes. We can also use the relative time delay between lensed events to better constrain the Hubble constant, which describes the rate of expansion of the universe. Lastly, gravitational lensing of GWs provides us with new ways of testing general relativity and allows us to study various relativistic systems[2].

While participating in the 2023 LIGO SURF program, I conducted research aimed at improving the detectors' search sensitivity in registering sub-threshold, strongly lensed events, where sub-threshold describes the lensed counterpart likely buried in the noise background. To accomplish this, I employed Bayesian hypothesis testing, comparing the posteriors of lens model dependent parameters, specifically the magnification factor and time delay, for the cases of lensing and no lensing. This was implemented as post-processing script in the gstLAL-based Targeted Subthreshold Lensing Search (TESLA) pipeline and returns the Bayes factor for a trigger using an already registered gravitational wave as the target lensed counterpart. In essence, a bivariate probabilities density is created from sample data obtained from a lens model, which is used in evaluating the likelihood real data in the search.

In this proposal, I provide background information on LIGO, gravitational waves, gravitational lensing, and the gstLAL and gstLAL-based TESLA search pipelines. I then further explain the objectives of this project and describe the methodology in accomplishing this research, including our implementation of Bayes theorem and the development of our hypothesis models. Finally, I share the results of this project and include closing remarks on future work to be done.

BACKGROUND

What is LIGO?

Short for Laser Interferometer Gravitational Wave Observatory, LIGO searches for gravitational wave signals coming from deep space, likewise making the smallest and most accurate measurements to date. Similar experiments began in the 1960s and, with the development and further improvement of interferometric detectors, LIGO's first detector was completed in the early 2000s. The (now updated) detectors are located in Hanford, Washington and Livingston, Louisiana, making them around 3000 kilometers in distance from each other, or 0.01 lightsecond. The detector's large separation helps determine any local noise (i.e. environmental or instrumental) and also helps confirm gravitational wave events when registered on both with the appropriate time delay. They also serve in measuring wave polarizations and source sky localizations [2]. To establish further confidence in these readings, the LIGO Scientific Collaboration (LSC) joined teams with Italy's VIRGO project in 2007. The next year, the National Science Foundation provided funding for Advanced LIGO, which became fully functional in 2015[3].

On September 14, 2015, during the first official observing run O1, both LIGO detectors simultaneously observed gravitational wave GW150914, making it the first direct detection of the phenomenon, which was predicted by Einstein's Gen-

eral Theory of Relativity using the nonlinear electrodynamics of black holes. Analysis showed GW150914 was in fact the coalescence of a binary black hole, which also marked the first observation of such an event.[2].

As of the second half of LIGO's third observing run (O3B), there's been a total of 90 observed events[4]. This includes the previously described GW150914[2] and GW170817, which was the gravitational wave emitted from a binary neutron star (BNS) merger and the largest registered GW signal to date, with a combined signal to noise ratio (SNR) of 32.4[5]. In comparison, GW150914 had a combined SNR of 24, although the VIRGO detector was not in operation at the time of the event[2].

Advanced LIGO operates using a modified Michelson interferometer, often called a Michelson-Morley interferometer. Each arm of the detector has a length of 4 km, necessary because a gravitational wave can produce displacements as small as 10^{-21}m. The detector's arms are placed in an L-shape because the compressions and expansions of spacetime caused by a GW are orthogonal, causing the arms to experience different amounts of displacement when a gravitational wave passes through. When this occurs, this difference in length is given by the equation

$$\Delta L(t) = \Delta L_x - \Delta L_y = h(t)L, \tag{1}$$

where $h(t)$ is the gravitational wave strain and L is arm length.[2]. However, instead of measuring displacements smaller than one-thousandth of a neutron, LIGO relies on the interference of light to detect such small changes. To do this, a laser beam is directed towards a beam splitter such that half of the beam is directed down one arm and the other half down the other arm. Each end has a mirror to reflect the beams, and the reflected beams recombine at the photodetector, which is set to have destructive interference when there is no GW present. When a GW passes through, the length of the arms change such that the recombined light instead produces constructive interference. There is also a Fabry-Perot power-recycling cavity that amplifies the power of the reflected wave from 20W to 100 kW, further helping the photodetector register the energy spike [2]. We measure this power output, which is really the phase difference between the recombined beams, and use transformation tools to derive the potential gravitational wave strain of the event. After this, we use further methods to determine if the signal is truly astrophysical in origin or if it simply noise mimicking signal.

What is a Gravitational Wave?

To understand gravitational waves, one must first realize the connection between space and time proposed by Einstein's General Theory of Relativity. Einstein began by exploring the relationship between gravitational mass, m_g, and inertial mass, m_i, which were simply assumed to be equal. Einstein did not make this assumption and instead worked on deriving the relationship from the bottom up. By studying the behavior of objects in a gravitational field, he realized that these two are equivalent only by accounting for the curvature of spacetime. This path is called a geodesic, and under this hypothesis, the equivalence of inertial and gravitational mass can be proven.

This led to the Equivalence Principle, which states that the only truly inertial state of an object in a gravitational field is in free-fall, or when it can move freely along its geodesic. This state of free-fall is called an inertial reference frame, or IRF. Instead of a force, Einstein proposed that gravity is a natural consequence of energy and mass interacting with spacetime, not each other. This is where the understanding of spacetime's fabric-like structure originates— the more massive an object is, the more it curves its specific region of spacetime. This ultimately led to the Einstein equation, which relates the geometry of spacetime to the distribution of matter and energy within it. This equation shows the interdependence between matter and spacetime or, as John Wheeler famously said, that "spacetime tells matter how to move and matter tells spacetime how to curve." Of course, the effects of a gravitational field cannot be completely dismissed for objects that aren't infinitesimally small. This is accounted for using tidal forces, which measures the stress/strain an object experiences while in a gravitational field. [6]

Because spacetime's geometry is dependent on the distribution of mass, accelerating objects will produce perturbations in spacetime that ripple outwards, known as gravitational waves. Anything with mass can produce gravitational waves, however most these waves are undetectable due to the large distances traveled or size of the source. Thus, we rely on detections from extremely massive, rapidly accelerating objects for gravitational wave analysis, such as neutron stars and black holes. Objects like lone neutron stars (i.e. non-binary with a constant spin) produce continuous gravitational waves caused by irregularities in their shape and, as the name suggests, these gravitational waves have frequencies and amplitudes that change very slowly with time.

Currently, continuous gravitational waves have not been detected, meaning LIGO's database contains only transitory gravitational wave events emitted from compact binary coalescence (CBC). There are many massive, extremely dense and rapidly accelerating bodies like neutron stars and black holes orbiting each other, known as binaries. Over time, these systems lose energy through gravitational radiation, which causes their orbital distance to shrink and their acceleration to increase. This initial phase is known as the inspiral phase of CBC and has relatively stable readings by the detectors. Eventually, the orbital frequency gets large enough to noticeably affect the readings of the emitted gravitational wave, showing a gradual increase in amplitude and GW frequency. When these massive objects join, there's an extreme surge in energy and the gravitational wave strain peaks, called the merger stage. After merging, the joint bodies move to the ringdown stage, which is defined as the event's end as the amplitude returns to zero. This three-step process is called compact binary coalescence, where compact describes extremely high-density objects. To better describe the specific system, these events

are divided into three subclasses: binary neutron star (BNS), binary black hole (BBH), and neutron star-black hole binary (NSBH) mergers. Gravitational waves produced by these binary systems will be the focus candidates of the project. We can use the frequency f and its time derivative $\dot{f}$ obtained from the the Fourier transform of the strain amplitude to derive their source parameters, such as chirp mass $\mathcal{M}_c$ (measured in solar masses) where m_1 and m_2 are the masses of each object in the binary and

$$\mathcal{M}_c = \frac{(m_1 m_2)^{3/5}}{(m_1 + m_2)^{1/5}} = \frac{c^3}{G}\left[\frac{5}{96}\pi^{-8/3} f^{-11/3}\dot{f}\right]^{3/5}. \quad (2)$$

In the case of GW150914, obtaining the chirp mass was essential in classifying the binary. Because $\mathcal{M} \approx 30M_\odot$, this meant $m_{net} = m_1 + m_2 \geq 70M_\odot$. Only a binary black hole system could have the combined mass and orbital frequency capable of this, as a BNS wouldn't have the necessary mass while and NSBH system would have a much smaller orbital frequency. This event had an orbital frequency of 75 Hz, which is always defined as exactly half the gravitational wave frequency[2].

As mentioned, when gravitational waves propagate, they stretch and squeeze spacetime orthogonally. This results in two different types of polarizations: plus polarization, h_+, when the perturbations occur vertically/horizontally and cross polarization, $h_\times$, when they occur diagonally. We use this information in determining how the GW affects the geometry of spacetime and in deriving information about the source event's parameters. The two different polarizations are shown in figure 2.

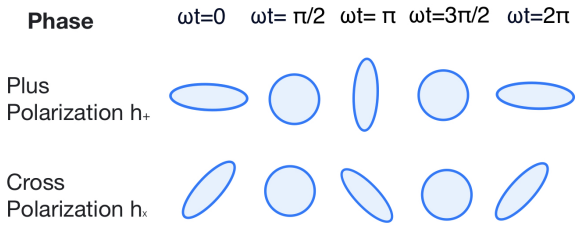

Figure 1. Diagram of h_+ and $h_\times$

What is Gravitational Lensing?

Now that we've realized spacetime's non-Euclidean geometry, we can better understand the behavior of light in the presence of a gravitational field. Fermat's principle states that light always travels the path requiring the shortest amount of time, however that path is now a curve (called a geodesic) rather than a straight line. When light traveling through space encounters a gravitational field, it bends to follow the curvature of the field's geodesic. This effect is known as gravitational lensing and, while there are similarities to traditional lenses, this lens results from spacetime's interaction with a massive body rather than the wave's interaction with a medium. General relativity states that anything with no inertial mass must travel at the speed of light, meaning gravitational waves behave similarly to light when passing through a gravitational field and thus experience the effects of lensing. In fact, the only difference in behavior is that gravitational waves are not altered by any medium whereas light encounters the interstellar medium as it travels to us. There are three classifications of gravitational lensing, which are described below in the context of light and gravitational waves.

Microlensing is the first type of lensing, which accounts for the lensing effects of less massive celestial objects, such as stars. When stars pass in front of each other, light from the background source is temporarily brighter. When this occurs, a single image is produced with very slight deviations from the original waveform. This concept is not limited to interactions between stars, as microlensing of light also helps us detect exoplanets by measuring the source star's change in brightness as an orbiting planet aligns with it and the observer. Microlensing occurs similarly in gravitational waves, although the effects are not directly detectable as the alteration in waveform is so small. LIGO considers microlensing in the context of unresolved gravitational waves in the data, which are collectively accounted for and termed stochastic background signal. This background can only be statistically analyzed, as the behavior of microlensing events in a population of smaller lenses such as stars contribute to this phenomenon. Some of these gravitational waves likely originate from the Big Bang, making this a noteworthy field of study as it could help us better understand the primordial universe.

Weak lensing occurs when the lens object is massive enough to deflect incoming light but doesn't have sufficient parameters to produce multiple images. Instead, the source image will appear distorted. For light, this results in a significantly brighter image. For gravitational waves, this results in a single, potentially detectable waveform that has a different SNR than the unlensed waveform. When LIGO detects continuous gravitational waves, we will be able to analyze this change in waveform directly using the unlensed signal. However, as we currently detect only CBC event, we again rely on statistical analysis to determine if weak lensing has occurred.

Strong lensing occurs when the lensing body is extremely dense and massive and thus produces two or more images of the source. These images are identical apart from their measured intensity caused by the path difference. When the source, lens and observer are perfectly aligned, this results in the phenomenon of Einstein rings and crosses, which occur for spherical and elliptical lensing objects respectively. In the context of gravitational waves, we expect two distinct gravitational wave events from CBC. Due to the path difference, these events will have identical waveforms apart from a change in amplitude, measured using a magnification factor derived from the SNRs, a time delay between the events and a morse phase factor that determines the overall phase shift in each lensed waveform. A shorter path corresponds an earlier arrival time and larger SNR, meaning the waveform's strain

amplitude appears magnified. Depending on the orientation of the source, lens and observer, lensed events can both be magnified with respect to the unlensed source event, both be demagnified, or be a combination.

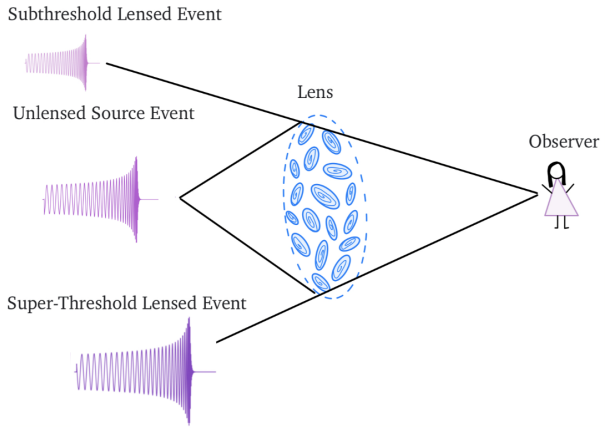

Figure 2. Strong lensing for a star forming galaxy

By assuming geometric optics, we're able to define the absolute time delay, change in SNR, or magnification, and morse phase $\Delta\phi$ for a pair of lensed signals with respect to the unlensed source event according to lens model. The morse phase describes the phase shift between the lensed and unlensed waveform, which is determined using the image type found from the solutions to the Fermat potential. Type I images are characterized by a phase shift of 0, type II a phase shift of $-\frac{\pi}{2}$, and type III a phase shift of $-\pi$. Together these describe any lensed counterpart with respect to the unlensed waveform as

$$\mathrm{h}^{lensed}(f,\bar{\theta},\mu,\Delta t,\Delta\phi) = \sqrt{\mu}\times\mathrm{h}^{original}(f,\bar{\theta},\Delta t)\times\exp(i\mathrm{sign}(f)\Delta\phi). \tag{3}$$

Given we have no way of analyzing an unlensed gravitational wave event for CBC, we instead determine the relative time delay and magnification factor between the two lensed events. Relative magnification is defined as the ratio of the lensed events SNRs ρ, or

$$\mu = \frac{\rho_{\text{trigger}}}{\rho_{\text{target}}}, \tag{4}$$

and the relative time delay is defined as

$$\Delta t = t_{\text{trigger}} - t_{\text{target}}. \tag{5}$$

What is a Lens Model?

The point-mass lens model is simplest way of analyzing gravitational lensing, which makes the assumption that the lens is simply a point mass. In this model, shown in figure 4, the wave travels along a straight line until it is bent by the lens, which causes an image to appear at a deflection angle, $\hat{\alpha}$, from the source. When c is set to unity, this angle is calculated as

$$\hat{\alpha} = \frac{4GM}{\xi}, \tag{6}$$

where G is the gravitational constant $6.67\times10^{-11}\ \frac{Nm^2}{kg^2}$ and ξ is the impact parameter, which is the closest approach of light for a given lens, and M is the mass of the lensing body.

By examining the equation, we see that $\hat{\alpha} \propto \frac{M}{\xi}$, meaning it depends only on the mass of the lens and the source's distance from the lens, measured orthogonal to the optical axis. Thus, the lensing effect becomes more pronounced as the deflection angle $\hat{\alpha}$ increases[7].

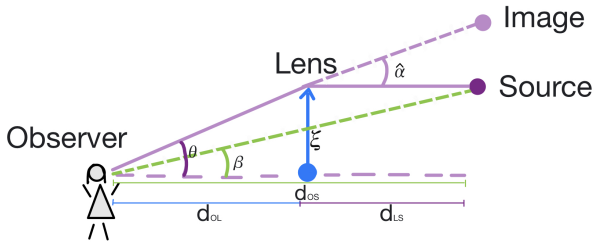

Figure 3. Point Mass Lens Model

If the source, lens and observer are perfectly aligned along the optical axis, infinitely many images form and are distorted into arcs that appear as a ring of light around the lens. The angular radius of an Einstein ring is given by the following equation:

$$\theta_E = \sqrt{4GM\frac{d_{LS}}{d_{OL}d_{OS}}} \tag{7}$$

When we assume small angles, $\sin(\theta) \approx \theta$ and $\xi = \theta d_{OL}$. Furthermore, we see that the image is at height θd_{OS}, which is equivalent to $\beta d_{OS} + \hat{\alpha} d_{LS}$. If we use to this to solve for θ, we see

$$\theta = \frac{\beta \pm \sqrt{\beta^2 + 4\theta_E^2}}{2} \tag{8}$$

There are two solutions to this equation, meaning we see multiple images. Because $\sqrt{\beta^2 + 4\theta_E} > \beta$, multiple images form when $\beta \neq 0$, one at an angle θ_+ above the optical axis and another at an angle θ_- below it. When $\beta = 0$, this equation breaks down into the equation for an Einstein ring's angular radius, in which there are an infinite number of images. If we solve the lens equation for the time-delay, there are three different solutions depending on the type lensed signal, called Type I, II and III lensed signals. They represent the minimum, saddle-point and maximum solutions, respectively. Type II images are Hilbert transform of the unlensed waveform, while Type I and Type III images are scaled versions of it. Type III images differ from Type I only by their sign.

In the case of LIGO, Type II images are prime candidates for detection given their similarity to the original waveform and consequential high SNR. This is because we assume geometric optics, in which waveform distortion only occurs when the image originates from a saddle-point solution[8].

However, the point-mass lens model fails in accounting for the mass distribution of the lensing galaxy. To approximate this better, we can instead employ the Singular Isothermal Sphere (SIS) model. The Singular Isothermal Ellipsoid (SIE) model is similar to the SIS model, although more realistic given it allows for elliptical symmetry of the lensing galaxy. Both of these models have singularities at their centers, meaning they fail in modeling cases of lensing where the light has the closest approach the lensing galaxy, which corresponds to type III images. In these cases, the Non-singular Isothermal Sphere or Ellipsoid (NSIS or NSIE) models are more appropriate. For even more massive lenses such as galaxy or dark matter clusters, models such as the Navarro-Frenk-White model work best. However, these are just a few of the many possible gravitational lensing models.

Identifying Triggers

When searching for transient gravitational waves, we must account for the various sources of noise that contribute to our measurements. Thus, the output data from the detectors, $d(t)$, is a combination of both noise, $n(t)$, and gravitational wave signal, $h(t)$, such that

$$d(t) = n(t) + h(t). \tag{9}$$

There are various types of noise affecting our data, including environmental noise (earthquakes, human activity, etc.) and thermal noise (the non-zero temperature of the interferometer). Because noise is a random process, we make the assumption that it is Gaussian and stationary to better approximate the power output for a given bandwidth of signal. We obtain the energy of a time-function by integrating over the square of the function's magnitude, which we can relate back to the frequency space using Parseval's theorem. This shows that the total energy in the time domain is equivalent to the total energy in the frequency domain, meaning both of these expressions are proportional to the power at a given point.

Because potential gravitational wave signals get buried underneath noise due to the incredibly small amplitude, we use various search pipelines to search for signal, all employing different methods of upranking signal. These measure the data using the signal-to-noise ratio (SNR), which describes the amplitude of the waveform or contributed arm strain. The optimal ρ is inversely proportional to the effective distance D_{eff} and, at detector's current sensitivity, events with an $\rho > 4$ are registered as a trigger.

Before we can run the data through a search pipeline, we must whiten it so the variance in amplitude is 1. If the amplitude of the data is higher than the variance (to a degree chosen by us), the pipeline disregards measurements in the ± 0.25s range, basically setting that interval's amplitude to 0. This process is called gating, and it's important we choose this degree so we minimize noise error specifically from glitches while not overlooking any potential GWs. We then perform the single-value-decomposition (SVD) to reduce the waveform templates into a set of basic vectors. After this, we decompose the template bank so only the necessary waveforms are kept, which reduces the computational time. To do this, we use each template's parameters to determine their time-frequency evolution, then split the template bank into partially-overlapping split-banks according to this. We then clip any overlapping regions so only distinct waveform templates remain, and again whiten the data. We also divide the split-banks into time-slices and set each template to have the same number of sample points. This is because lower frequencies have more templates and are likewise susceptible to oversampling. Finally, SVD is again performed, now returning the most important basis waveform.

The gstLAL search pipeline works by calculating the Bayes factor, or the likelihood ratio of the signal's template waveform parameters being astrophysical versus them being noise. This is defined as

$$\mathcal{L} = \frac{\mathcal{L}(\vec{O}, \vec{D_H}, \vec{\rho}, \vec{\xi^2}, [\Delta\vec{t}_{\text{coinc}}, \Delta\vec{\phi}_{\text{coinc}}]|\text{signal})}{\mathcal{L}(\vec{O}, \vec{D_H}, \vec{\rho}, \vec{\xi^2}, [\Delta\vec{t}_{\text{coinc}}, \Delta\vec{\phi}_{\text{coinc}}]|\text{noise})} \times \frac{\text{P}(\vec{\theta}|\text{signal})}{\text{P}(\vec{\theta}|\text{noise})}. \tag{10}$$

This is described by the template parameters are the participating detectors $\vec{O}$, the maximum horizon distances for each detector (or their sensitivity) $\vec{D}_H$, their matched-filter signal-to-noise ratio $\vec{\rho}$, their auto-correlation based signal consistency test values $\vec{\xi^2}$, and the time and phase delay between coincident events Δt_{coinc} and $\Delta\vec{\phi}_{\text{coinc}}$. The ratio of P($\vec{\theta}$|signal) and P($\vec{\theta}$|noise) represents how likely the template parameters are to model the trigger given it's GW signal or noise. We can calculate the False-Alarm-Rate to determine the event's significance, which gives a measure of how often noise can mimic the given waveform. The gstLAL then ranks candidate events according to this. A smaller FAR means a lower likelihood of the candidate being produced by noise, thus increasing the likelihood of it being a real gravitational wave signal. Candidates are selected for further analysis if they go above a threshold decided by the analyst. This gives us a ranked list of possible candidates as well as the source parameters of the templates that identified them. However, source parameters can differ widely from the template parameters, so this list only serves in identifying candidates worthy of follow up analysis, not as a method of determining the actual source parameters. [9].

One method of determining statistical significance is the coincidence criterion. Because there are multiple detectors with fixed locations, we can determine the time-frame in which the detectors should register the same gravitational wave signal. For example, because the LIGO Hanford and LIGO Livingston detectors are 0.01 light-seconds apart, their respective triggers for the same event should also occur within this

general time-frame. However, because that time interval is specific to light, we increase the coincident time interval by a small amount to account for uncertainties in the GW's behavior. The gstLAL also enforces coincident triggers to have the same parameters, and together this information is used in determining the event's statistical significance. Now non-coincident triggers are marked as noise, which helps us better understand the probability density of each detector's noise background.

Searching for Lensed Pairs

Although this method is sufficient in detecting gravitational waves, it may fail in detecting sub-threshold lensed counterparts because they have low ranking statistics and are more easily buried in the noise background. However we can remedy this using the gstLAL-based TargetEd Sub-Threshold Lensing SeArch pipeline (TESLA). With TESLA, we take the known information about the super-threshold candidate and reduce the template bank so only templates with reasonable source parameters remain. Because the source parameter estimation of the super-threshold GW gives us a probability distribution rather than a fixed value, we also obtain the proper parameter estimation for the sub-threshold event using the Bayesian posterior probability distribution. This helps in reducing background noise while keeping the relevant template waveforms. If the noise is Gaussian and stationary, keeping only the space enclosed by the 90% credible region is sufficient in covering the sub-threshold counterparts. Yet most noise is non-Gaussian and a leading cause of false alarms, so this region is insufficient in searching for the targeted GW. Thus, research aims at decreasing the amount of templates picking up unwanted background noise while keeping the templates necessary in picking up the desired foreground information, i.e. the most probable template parameters.

This leaves us to decide what regions of the parameter space should be targeted, which is done by injecting samples of the sub-threshold signal and keeping only the templates that recover them using the gstLAL. To register as a trigger, it still requires an $\rho > 4$ so we tweak one of the original parameters to simulate lensed signal. Because the source's effective distance D_{eff} is inversely proportional to the SNR, we can demagnify the confirmed waveform SNRs by increasing the measured effective distance. During an injection period, there is one injection with the original SNR and 9 weaker injections to describe the SNRs at the increased effective distances. The weaker injections are determined so the weakest injection registers an $\rho \geq 4$ in all detectors. We then inject the signals into our data and run them through the gstLAL with a full template bank, keeping templates capable of recovering the injections and adding them to the reduced template bank. The results are then analyzed so templates that significantly deviate from our original source parameter's posterior space are discarded. We then use this reduced template bank to search for potential sub-threshold lensed counterparts within all possible data. After this, we create a priority ranking list using the FAR ranking statistics from the confirmed gravitational wave. As with traditional analysis, this gives the likelihood of the signal being astrophysical, not of it being a lensed counterpart. Overall, the TESLA method maximizes the efficiency of the search by producing a nearly optimal template bank and reduces the noise background by accounting for glitches. This process is again described in figure 5 below [9].

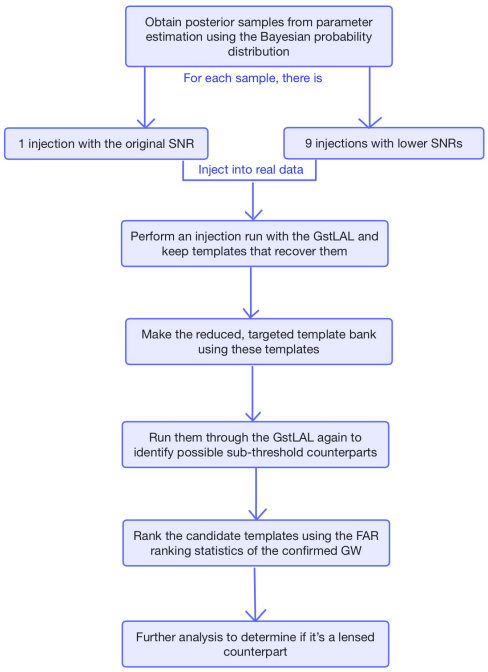

Figure 4. TESLA flowchart for a given target event

A test performed on the two LIGO detectors and the VIRGO detector using data from GW220112a showed that the TESLA template bank is the most effective in searching for sub-threshold counterparts. When compared to a single template bank containing the posterior samples from the target event with maximum probability, a PE template bank containing templates in the posterior probability distribution's 90% credible region and a template bank selected at random, the TESLA bank found $+9.26\%$ more injections than the general search. In comparison, the single, PE and random template bank missed more injections than the general search, having found percent changes of -40.0%, -80.3% and -77.5% respectively. Because the PE template bank only considers noise for the super-threshold event, it's more likely to miss the sub-threshold event due to the time delay. The TESLA template bank takes into account the signal sub-space of the confirmed event and glitches, making it more likely to recover the lensed counterparts[9].

METHODOLOGY AND RESULTS

The overall objective of this project was incorporating the relative time delay and magnification distributions predicted by lens models into ranking possible sub-threshold, strongly-lensed candidates. This provides us with a lensed likelihood based on the type of lens model used and super-threshold event in question. We use this with the parameters' likelihood for the case of no lensing to determine the Bayes factor, which can then be used in statistical analysis for gravitational lensing with real data. This is incorporated as post-processing script in the gstLAL-based TESLA search pipeline.

The gstLAL search pipeline uses Bayesian hypothesis testing to determine if the signals are either astrophysical or noise. The proportional form of Bayes theorem is given as

$$\mathrm{P(hypothesis|data)} \propto \mathcal{L}(\mathrm{data|hypothesis}) \times \mathrm{p(hypothesis)} \tag{11}$$

We search for the posterior, which represents how likely the hypothesis is given the data. $\mathcal{L}$(data|hypothesis) is the likelihood of seeing the data given the hypothesis, p(hypothesis) is the prior, or our initial belief. When find the equivalent form, the right hand side is divided by the evidence about data, E(data). Unless working on model selection, the evidence is used only as a normalization constant and set equal to the integral of the numerator from $-\infty$ to ∞. This means the area under the curve of the probability distribution function always equals 1. However, given that we're calculating the ratio of the likelihoods, we may ignore the evidence because the it's the same for both hypotheses.

When comparing two hypotheses, we can take the ratio of the proportional form of their posteriors if using the same data, or when the two evidence terms are equal. This allows us to measure how strongly one hypothesis explains the data in comparison to another, given by the equation

$$\frac{\mathrm{P(hypothesis_1|data)}}{\mathrm{P(hypothesis_2|data)}} = \frac{\mathcal{L}(\mathrm{data|hypothesis_1}) \times \mathrm{p(hypothesis_1)}}{\mathcal{L}(\mathrm{data|hypothesis_2}) \times \mathrm{p(hypothesis_2)}}. \tag{12}$$

In creating the post-processing script to search for lensed signals, we employed Bayesian hypothesis testing, comparing the lensed versus unlensed hypotheses for a trigger. We define the posterior odds $O^{\mathrm{lensed}}_{\mathrm{unlensed}}$ as

$$O^{\mathrm{lensed}}_{\mathrm{unlensed}} = \frac{\mathcal{L}(\mu, \Delta t|\mathrm{lensed})}{\mathcal{L}(\mu, \Delta t|\mathrm{unlensed})} \times \frac{\mathrm{p(lensed)}}{\mathrm{p(unlensed)}}. \tag{13}$$

This new likelihood ratio, or Bayes factor, compares the likelihood of seeing the given parameters for two hypotheses and is defined as

$$\mathcal{L}^{\mathrm{lensed}}_{\mathrm{unlensed}} = \frac{\mathcal{L}(\Delta t, \mu|\mathrm{lensed})}{\mathcal{L}(\Delta t, \mu|\mathrm{unlensed})}. \tag{14}$$

This is value is a stronger measure of the results as prior odds can often differ depending on one's approach. As mentioned, the time delay Δt represents the difference between the geocenter end times of the subthreshold and super-threshold event, making it independent of the time delay experienced by detectors. The magnification μ is defined as the ratio between the trigger and target event SNRs ρ. In this project, we primarily worked on modeling the numerator of the likelihood ratio, or the likelihood that an event with parameters μ and Δt values is lensed. To do this, we employed Gaussian kernel density estimation (KDE). The script incorporates user-provided sample points containing values for the relative time delay and magnification values according to a given lens model and then performs KDE over the two-dimensional data set to build unique probability density functions according to input. The figure below shows the bivariate probability density function for sample data obtained from an SIE lens model when considering a pair of type I and type II images.

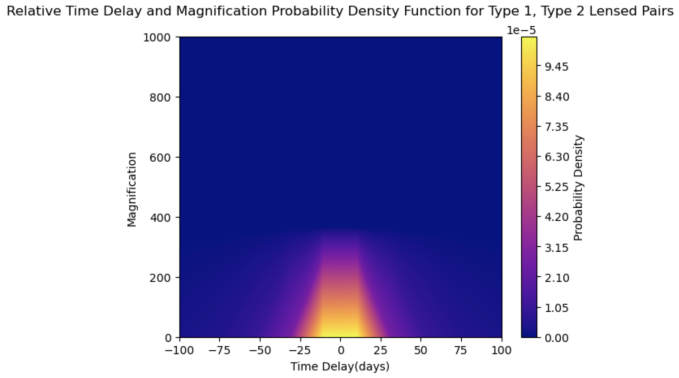

If we isolate each parameter's probability density function, they appear as follows.

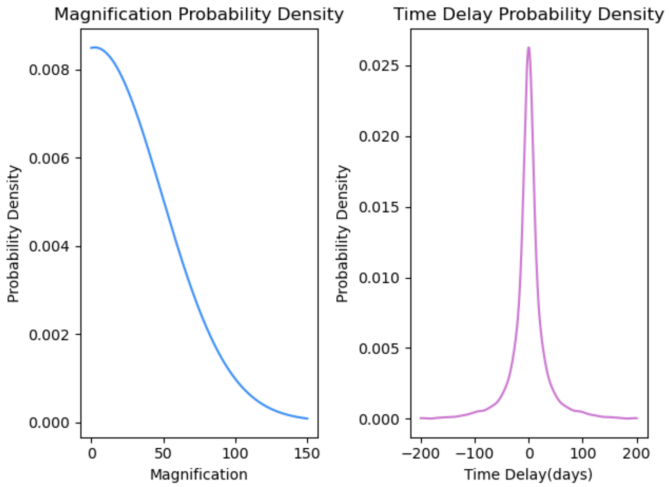

We see that the most likely value for magnification is somewhere around 1, while the most likely time delay value is very small, lying somewhere near 0. The models serve in assigning probability density values for parameters when considering real data.

When incorporating the denominator into the likelihood calculation, we considered the each probability density function individually as they're independent for both lensing and

no lensing. The likelihood of seeing a given time delay provided the signal is not lensed has been previously calculated as

$$\mathcal{L}(\Delta t|\text{not lensed}) = \frac{2}{T}(1 - \frac{\Delta t}{T}), \tag{15}$$

where T describes the livetime of the detectors, or how long they have been operating for the given observing run, and Δt represents the time delay between two randomly selected, unlensed events[10]. To calculate the likelihood of the magnification for the unlensed hypothesis, we used rejection sampling with red-shift as a model to obtain

$$\text{P}(\mu|\text{not lensed}) = \left(\frac{d_L^a}{d_L^b}\right)^2. \tag{16}$$

In this, we used the relationship between red-shift and luminosity distance, and luminosity distance and SNR to determine the magnification probability density using pairs of randomly selected, unlensed events.

While the prior odds is not currently used in the script, it can be understood as the expected rate of strong lensing within LIGO's observational range. For the case of lensing, we have an informed prior, meaning it is dependent on the true source red-shift. As this value increases, so does the expected rate of lensing. However, this value is extremely small, and can be approximated as somewhere between 10^{-3} to 10^{-4} events per year[11].

When running the lensing search script, we get the traditional rankings for astrophysical signal determined during the gstLAL/TESLA search in addition to new data describing the lensing likelihood ratio. This is determined for three different models: type I and type II pairs, type I and type I pairs, and type II and type II pairs. We also include a marginalized likelihood which averages over these three models. We see this graphically as an inverse event count, shown for type II pairs in the figure below.

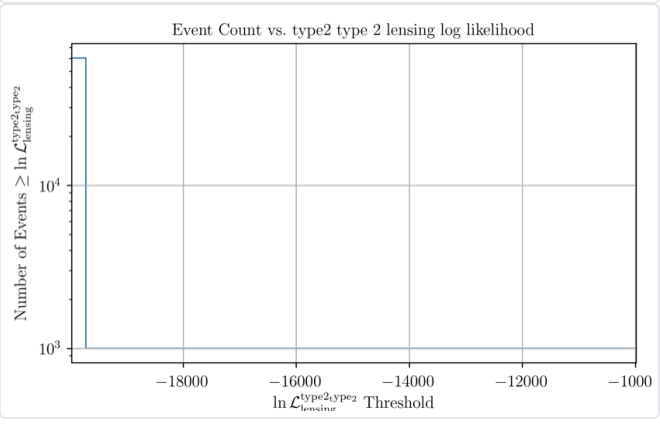

CONCLUSIONS AND OUTLOOK

With more gravitational waves to be detected in LVK's upcoming observing run, we have increasing chances of making the first detection of strongly lensed gravitational waves. Hence, it is crucial to boost the search sensitivity of existing search pipelines for strongly lensed gravitational wave, superthreshold or subthreshold, as much as possible. In this research, we investigated and implemented a lensing likelihood term to triggers found from TESLA, a targeted sub-threshold search pipeline for strongly lensed gravitational waves. The lensing likelihood evaluates the ratio of probabilities of obtaining a relative time delay and magnification compared to a target super-threshold gravitational wave for each trigger, under the lensed and unlensed hypothesis respectively. The goal of evaluating this likelihood is to provide an initial priority ranking for candidates coming from the TESLA pipeline for lensing follow-up analysis. To fully access the success of this search, we must inject data containing the lensing parameters for unlensed wave- forms. This will gives us a threshold for determining the significance of the lensing likelihood ratio when searching for lensed events in real data. Currently, the gstLAL returns closed and open box methods of analyzing the likelihood for noise and signal. For the latter, the event count shows a devi- ation from the expected noise curve when a signal is present. Our goal is to create a similar representation for the event count of potential lensed signals, where unlensed signal is used as a model curve instead of noise.

ACKNOWLEDGEMENT

I would like to thank my mentors Professor Alan Weinstein and Alvin Li. We would like to thank the LIGO Laboratory and Caltech Student Faculty Programs office for the opportunity to participate in this SURF and WAVE programs and for their support throughout the summer. We thank the NSF REU program for their support.

[a] haleyboswell@live.com

[1] L. S. Collaboration and V. Collaboration, arXiv (2021), arXiv:2105.06384.
[2] B. et al., PHYSICAL REVIEW LETTERS **116**, 061102 (2016).
[3] R. W. Kip Thorne, "A brief history of ligo," .
[4] LSC, "O3b catalog," .
[5] B. et al., PHYSICAL REVIEW LETTERS **119**, 161101 (2017).
[6] T. A. Moore, *A General Relativity Workbook* (2012).
[7] LibreTexts, ed., *Big Ideas in Cosmology*.
[8] A. K. L. Y. C. Yijun Wang, Rico K.L. Lo, arXiv (2021), arXiv:2101.08264v2.
[9] S. S. C. C. E. L. T. G. F. L. A. J. W. Alvin K. Y. Li, Rico K. L. Lo, arXiv (2022), arXiv:1904.06020v6.
[10] I. M. H. Rico K. L. Lo, arXiv (2021), arXiv:2104.09339.
[11] T. L. S. Collaboration and the Virgo Collaboration, arXiv (2021), arXiv:2105.06384.